The Journal of Clinical Endocrinology & Metabolism, 2021, Vol. 106, No. 2, e966–e981
doi:10.1210/clinem/dgaa803
Clinical Research Article

Clinical Research Article

Identification and Metabolic Profiling of a Novel Human Gut-derived LEAP2 Fragment

Christoffer A. Hagemann,[1,2] Chen Zhang,[1] Henrik H. Hansen,[1] Tina Jorsal,[2] Kristoffer T. G. Rigbolt,[1] Martin R. Madsen,[1] Natasha C. Bergmann,[2] Sebastian M. N. Heimbürger,[2,3] Mechthilde Falkenhahn,[4] Stefan Theis,[4] Kristin Breitschopf,[4] Stephanie Holm,[5] Morten A. Hedegaard,[5] Mikkel B. Christensen,[2,6,7] Tina Vilsbøll,[2,3,6] Birgitte Holst,[5,8] Niels Vrang,[1] Jacob Jelsing,[1] and Filip K. Knop[2,3,6,8]

[1]Gubra Aps, 2970 Hørsholm, Denmark; [2]Center for Clinical Metabolic Research, Gentofte Hospital, University of Copenhagen, 2900 Hellerup, Denmark; [3]Steno Diabetes Center Copenhagen, 2820 Gentofte, Denmark; [4]Sanofi Aventis, 65929 Frankfurt, Germany; [5]Department of Biomedical Sciences, University of Copenhagen, 2200 Copenhagen, Denmark; [6]Department of Clinical Medicine, Faculty of Health and Medical Sciences, University of Copenhagen, 2200 Copenhagen, Denmark; [7]Department of Clinical Pharmacology, Bispebjerg Hospital, University of Copenhagen, 2400 Copenhagen, Denmark; and [8]Novo Nordisk Foundation Center for Basic Metabolic Research, Faculty of Health and Medical Sciences, University of Copenhagen, 2200 Copenhagen, Denmark.

ORCiD numbers: 0000-0002-3732-0281 (H. H. Hansen); 0000-0001-7432-097X (B. Holst); 0000-0002-3845-3465 (F. K. Knop).

Received: 12 August 2020; Editorial Decision: 26 October 2020; First Published Online: 2 November 2020; Corrected and Typeset: 15 December 2020.

Abstract

Context: The mechanisms underlying Roux-en-Y gastric bypass (RYGB) surgery-induced weight loss and the immediate postoperative beneficial metabolic effects associated with the operation remain uncertain. Enteroendocrine cell (EEC) secretory function has been proposed as a key factor in the marked metabolic benefits from RYGB surgery.

Objective: To identify novel gut-derived peptides with therapeutic potential in obesity and/or diabetes by profiling EEC-specific molecular changes in obese patients following RYGB-induced weight loss.

Subjects and Methods: Genome-wide expression analysis was performed in isolated human small intestinal EECs obtained from 20 gut-biopsied obese subjects before and after RYGB. Targets of interest were profiled for preclinical and clinical metabolic effects.

Results: Roux-en-Y gastric bypass consistently increased expression levels of the inverse ghrelin receptor agonist, liver-expressed antimicrobial peptide 2 (LEAP2). A secreted endogenous LEAP2 fragment ($LEAP2_{38-47}$) demonstrated robust insulinotropic properties, stimulating insulin release in human pancreatic islets comparable to the gut hormone glucagon-like peptide-1. $LEAP2_{38-47}$ showed reciprocal effects on growth hormone secretagogue receptor (GHSR) activity, suggesting that the insulinotropic action of the peptide may be directly linked to attenuation of tonic GHSR activity. The fragment was

ISSN Print 0021-972X ISSN Online 1945-7197
Printed in USA

infused in healthy human individuals (n = 10), but no glucoregulatory effect was observed in the chosen dose as compared to placebo.

Conclusions: Small intestinal LEAP2 expression was upregulated after RYGB. The corresponding circulating $LEAP2_{38-47}$ fragment demonstrated strong insulinotropic action in vitro but failed to elicit glucoregulatory effects in healthy human subjects.

Freeform/Key Words: obesity, bariatric surgery, enteroendocrine cells, gut hormone, liver-expressed antimicrobial peptide 2, peptide fragment

The obesity pandemic has increased the number of people undergoing bariatric surgery, eg, Roux-en-Y gastric bypass (RYGB), which in addition to robust and sustained weight loss improves glycemic control in or even causes remission of type 2 diabetes (1–3). Roux-en-Y gastric bypass entails the rerouting of nutrients through a small gastric pouch directly into the jejunum, thus bypassing the major part of the stomach and the duodenum. An increasing body of evidence suggests that RYGB triggers multifactorial mechanisms involved in metabolic control. A striking feature of RYGB is the rapid improvement in glycemic control that precedes weight loss, which has been associated with reduced hepatic insulin resistance and increased pancreatic beta-cell sensitivity in response to caloric restriction (4). With accompanying robust weight loss, improved insulin sensitivity in muscle and adipose tissue contributes to improved glycemic control in RYGB patients (5, 6). Roux-en-Y gastric bypass patients show distinct serum metabolome profiles suggesting altered amino acid and lipid metabolism (7, 8). The metabolic signatures have been linked to shifts in bile acid and gut microbiome profiles, which may contribute to the positive metabolic outcomes of RYGB (9, 10). Notably, adaptive changes in gut-derived signals are considered a key mechanism in both the immediate and long-term therapeutic effects of RYGB. As for the postabsorptive metabolic changes, exaggerated postprandial gut hormone responses likely result from the accelerated passage and absorption of nutrients in the small intestine. Accordingly, absorption of nutrients constitute a powerful stimulus for hormone secretion from enteroendocrine cells (EECs) (11, 12). Numerous studies have demonstrated alterations in circulating gut hormone profiles in RYGB patients. Robust postprandial increases in gut hormones with a documented role in glucoregulatory control and satiety signaling, such as glucagon-like peptide 1 (GLP-1), peptide YY, and cholecystokinin, have been reported (6, 13–15). Roux-en-Y gastric bypass-induced weight loss has also been associated with elevated levels of other appetite-suppressing gut hormones, including oxyntomodulin and neurotensin (13, 16). Roux-en-Y gastric bypass patients exhibit transiently reduced circulating levels of the gastric orexigenic hormone ghrelin, suggesting that impaired postprandial ghrelin secretory capacity may be involved in the initial decrease in appetite (17, 18). In contrast, inconsistent effects on obestatin levels, another hormone encoded by the ghrelin gene with controversial anorectic effects, have been reported after RYGB-induced weight loss (19, 20).

Studies replicating postprandial gut hormone levels after RYGB have supported the concept that synergistic effects of secreted gut peptides may be an important mechanism for the glycemic improvements, appetite suppression, and weight loss benefits from surgery (21, 22). As RYGB is established as the most efficacious treatment for obesity and type 2 diabetes, attempts have been made to provide medical "gastric bypass mimetics" using specific combinations of gut hormone analogs (23). Despite the wealth of potential mediators of RYGB-induced metabolic benefits, the exact mechanisms are far from well-understood, and several other and unknown contributors may exist. Anatomical and transcriptional changes in EECs have been proposed as an important mechanism for increased postprandial gut hormone secretion following RYGB surgery (24–27). Therefore, a deeper understanding of RYGB-induced regulatory changes in EEC preprohormone genes and secreted peptide products may disclose new therapeutic targets for obesity and diabetes.

In the present study, genome-wide expression patterns in EECs were determined from human gut biopsies obtained during and after RYGB, with the aim to identify and characterize novel gut-derived peptides with therapeutic potential in obesity and/or diabetes. Liver-expressed antimicrobial peptide 2 (LEAP2) mRNA levels were consistently upregulated in human EECs following RYGB, while fasting and postprandial circulating LEAP2 concentrations remained unchanged. LEAP2 has recently been proposed as a novel regulator of food intake and body weight through its reciprocal relationship to ghrelin (28). LEAP2-related peptide fragments have been demonstrated to act as inverse ghrelin receptor agonists, which could potentially implicate LEAP2 degradation products in metabolic control (29). Interestingly, a secreted endogenous LEAP2 fragment ($LEAP2_{38-47}$) was detected in RYGB patients. $LEAP2_{38-47}$ demonstrated insulinotropic properties in vitro, promoting an increase in insulin release nearly

comparable to GLP-1. The insulin secretagogue characteristics were consistent with $LEAP2_{38-47}$, acting as an inverse ghrelin receptor agonist. When infused intravenously in healthy human subjects, the chosen dose did not exhibit insulin secretory or glucoregulatory effects, suggesting that $LEAP2_{38-47}$ may not play an important role in glycemic control.

Materials and Methods

Ethical considerations

The human studies were approved by the Scientific-Ethical Committee of the Capital Region of Denmark (registration numbers H-6-2014-047 and H-18027152). The human studies were conducted in accordance with the Declaration of Helsinki (7th revision, 2013) and all participants gave informed consent prior to inclusion. All animal experiments were conducted according to international accepted principles for care and use of laboratory animals and were covered by a license issued by The Animal Experiments Inspectorate, Denmark (2013-15-2934-00784).

Tissue sampling in individuals undergoing RYGB surgery

A prospective observational study of morbidly obese individuals referred to elective RYGB surgery at a Danish public hospital was carried out at the Center for Clinical Metabolic Research, Gentofte Hospital, University of Copenhagen between December 2014 and December 2016. The study population and experimental design has previously been described in detail (30). The study was registered at ClinicalTrials.gov (reg. no. NCT03093298). In total, 20 obese participants (5 males, 15 females) participated in the study (baseline characteristics: age (median [interquartile range]) 46.5 [39.0–50.8] years, body mass index 40.3 [36.3–43.6] kg/m^2, hemoglobin A1c 33 (31–34) mmol/mol. At time of inclusion, 3 participants were diagnosed with type 2 diabetes and treated with metformin monotherapy, which was discontinued 7 days prior to experimental days. A perioperative gut biopsy was sampled (approximately 1-cm gut segment) from the jejunal division site. Postoperative mucosal biopsies were sampled from the alimentary limb, biliopancreatic limb, and common channel, respectively, using a pediatric colonoscope (PCF-Q180AL; Olympus, Tokyo, Japan) during propofol sedation (Fig. 1). Immediately after sampling, biopsies were embedded in Tissue-Tek (Sakura Finetek, Torrance, California), snap-frozen in liquid nitrogen and stored at -80°C until analysis. A part of the perioperative gut biopsy was dissected and fixated in 10% neutral buffered formalin.

Mixed meal tolerance tests before and after RYGB

During study enrolment, all participants underwent 3 sequential liquid mixed meal tests (MMTs) after overnight fasting at 1 week (-1.1 ± 0.1 w) before as well as 1 week (+1.3 ± 0.1 w) and 3 months (+12.0 ± 0.3 w) after RYGB surgery. The liquid mixed meal consisted of a 200 mL Nutridrink (300 kcal, carbohydrate [50 kcal%], protein [15 kcal%], fat [35 kcal%]; Nutricia Nutridrink, Allerød, Denmark) ingested evenly over a 30-minute period (time 0–30 minutes). Blood samples were collected from an intravenous catheter inserted into an antecubital vein at time points 0, 30, 60, 120, and 240 minutes. The arm for blood sampling was wrapped in a heating pad (45°C) to arterialize the venous blood. Blood was collected in chilled P800 K_2EDTA tubes containing a cocktail of protease, esterase, and dipeptidyl peptidase-4 inhibitors (#366420; BD Biosciences, San Jose, California), centrifuged 15 minutes (2900 g, 4°C), and stored at -80°C until analysis.

Laser capture microdissection and RNA sequencing

Laser capture microdissection (LCM) was used to sample epithelial cells positive for CgA staining, a marker for endocrine cells (31), in perioperative (n = 19) as well as postoperative biopsies (alimentary limb, n = 18; biliopancreatic limb, n = 18; common channel, n = 20).

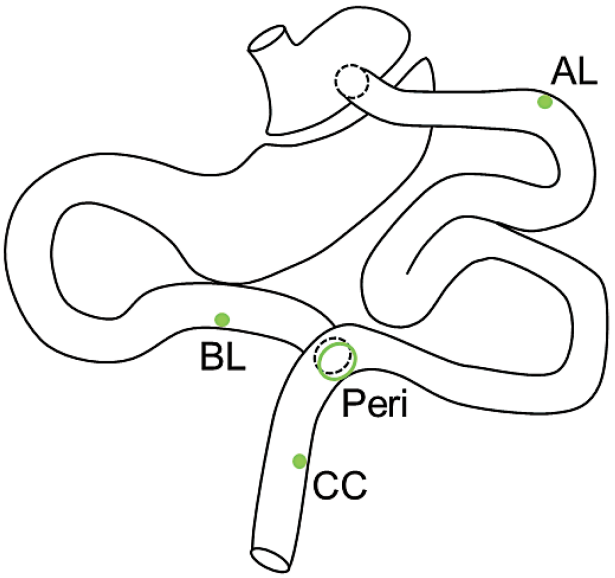

Figure 1. Sampling scheme in obese individuals undergoing RYGB surgery. Peri- and postoperative sampling sites for gut biopsies from morbidly obese individuals undergoing RYGB surgery. Abbreviations: AL, alimentary limb; BL, biliopancreatic limb; CC, common channel; Peri, perioperative; RYGB, Roux-en-Y gastric bypass.

Frozen gut mucosal biopsies were sectioned into 8-µm cryosections (at -20°C) using a cryostat (CM 3050S; Leica Biosystems, Wetzlar, Germany) onto precooled RNAase-free Superfrost slides (VWR, Søborg, Denmark). Sections were stored at -80°C until further processing. Enteroendocrine cells were identified using a CgA primary Ab (#ab45179; Abcam, Cambridge, UK) diluted 1:50 in 2 M NaCl phosphate-buffered saline (PBS) and a secondary rabbit antimouse Ab diluted 1:1 in 4 M NaCl PBS (#RHRP520; Biocare Medical, Pacheco, California). After rinsing in 2 M NaCl phosphate buffered saline, 100 µL of fluorescein isothiocyanate tyramide signal amplification reagent (1:100, diluted in 2 M NaCl PBS with 0.0015% H_2O_2) was applied. Prior to single-cell LCM, CgA-stained slides were subjected to a series of dehydration and delipidation steps. Laser capture microdissection was performed using Veritas LCM equipment and CapSure Macro caps (Life Technologies, Carlsbad, California). Individual cells were collected by use of the infrared capture laser only, ie, collected without cutting). A total of 1000 CgA-positive cells were collected from each biopsy and processed for RNAseq, as described in detail previously (32). The RNA integrity number ranged from 5.0–7.7 (mean 6.4). RNAseq libraries were prepared using Illumina TruSeq Stranded mRNA Library Prep kit (#20020594; Illumina, San Diego, California) and sequenced on a NextSeq 500 sequencing instrument (Illumina, San Diego, California). Samples were sequenced with an average sequencing depth of 37 million reads per sample. Reads were mapped to the GRCh38.p10 Ensembl human genome using STAR v.2.5.2a with default parameters. The R package DESeq2 v.1.18.1 was used for differential expression analysis (33). Genes below a raw count of 10 were excluded from the analysis. Genes with a Benjamini and Hochberg adjusted $P < 0.05$ (5% false discovery rate) were regarded as statistically significantly regulated. Differentially expressed preprohormone genes were extracted from the RNAseq data set using characteristics specific to prohormones (presence of secretory signal peptide, prohormone length less than 270 aa, absence of transmembrane segments, proprotein convertase cleavage site [KK, KR, RK, RR], modular domains, and compositional bias). RNAseq data is available through the Gene Expression Omnibus (GEO) database (34).

Detection of LEAP2 in plasma before and after RYGB surgery

LEAP2 plasma concentrations were determined by use of a LEAP2 enzyme immunoassay specific for the human ($LEAP2_{38-77}$) and mouse ($LEAP2_{37-76}$) peptide (#EK-075-40; Phoenix Pharmaceuticals, Burlingame, California), according to the manufacturer's instructions. In brief, 50 µL of standards, positive control, and human plasma samples (diluted 1:50 in 1 × assay buffer) were loaded in duplicates on a secondary antibody precoated 96-well immunoplate. Subsequently, 25 µL of primary Ab and 25 µL biotinylated peptide were added to each well (except the blank wells) and plates were incubated for 2 hours at room temperature. After 4 × washes with 1 × assay buffer, 100 µL Streptavidin-horseradish peroxidase (HRP) concentrate was added to each well and the plate was incubated for 1 hour at room temperature. After 4 × washes with 1 × assay buffer, 100 µL 3,3′,5,5′-Tetramethylbenzidine substrate solution was added to each well and incubated for 1 hour at room temperature. The reaction was terminated by adding 100 µL of 2 M Hydrogen chloride to each well. The absorbance was measured at 450 or 590 nm and plasma concentrations of LEAP2 were extrapolated from the standard curve. All positive controls remained within the quality range.

In situ hybridization analysis of LEAP2 mRNA distribution in human gut biopsies

Formalin-fixed perioperative gut biopsy samples were paraffin-embedded and cut into 5-µm sections onto Superfrost Plus Slides. For comparison to mouse LEAP2 mRNA distribution, gut sections from C57Bl6/J mice were included. Slides for in situ hybridization (ISH) were stored at -20°C until further processing. ISH was performed using the RNAscope 2.0 High Definition RED Assay (#310036; Advanced Cell Diagnostics, Hayward, California) using human LEAP2-specific probes and the HybEZ Hybridization System (#310013; Advanced Cell Diagnostics, Hayward, California), according to the manufacturer's instructions. ISH signals were detected with Fast-RED and counterstained with Gill's hematoxylin, and virtual images were obtained using an Aperio ScanScope Scanner (Leica Biosystems, Wetzlar, Germany). A negative (Bacillus Subtillis, dihydropicolinate reductase; EF191515) ISH control probe was employed for assay validation in all analyses.

Immunohistochemical analysis of $LEAP2_{38-47}$ expression in human gut biopsies

Immunohistochemical stainings were performed on deparaffinized, formalin-fixed human jejunal sections. Antigen retrieval was achieved by boiling the slides in triethylene glycol buffer (10 minutes, pH 9.0), rinsed in tris-buffered saline (TBS) with 0.05% Tween 20 (TBS-T) (3 × 3 minutes). Endogenous peroxidase activity was blocked by incubating slides in 1% H_2O_2 in TBS for 10

minutes and then rinsed in TBS-T for 2 × 3 minutes. Slides were then blocked with blocking buffer (TBS-T + 5% swine serum + 1% bovine serum albumin [BSA]) for 20 minutes and incubated for 1 hour with primary rabbit anti-$LEAP2_{38-47}$ Ab (1:300, #5999; GenScript, Piscataway, New Jersey). Sections were rinsed in TBS-T buffer and incubated for 30 minutes in Anti-Rabbit EnVision+ HRP labeled polymer (K4003; Agilent-Dako, Glostrup, Denmark). Following rinses in TBS-T buffer, sections were incubated with 3,3′diaminobenzidine solution (K3468; Agilent-Dako, Glostrup, Denmark) for 10 minutes. Sections were dehydrated, counterstained in hematoxylin, and finally coverslipped. For dual IHC, slides were incubated in blocking buffer for 20 minutes (5% swine serum in TBS-T added 1% BSA) and with primary antibodies (rabbit anti-$LEAP2_{38-47}$, 1:400, #5999, GenScript, Piscataway, New Jersey; mouse CgA 1:50, #ab8204, Abcam, Cambridge, UK) diluted in blocking buffer added 1% BSA for 60 minutes. After rinsing in TBS-T (3 × 3 minutes), Envision+ HRP-Polymer antirabbit (#K4003; Agilent Dako, Glostrup, Denmark) was added for 30 minutes. Slides were rinsed in TBS-T (3 × 3 minutes) and incubated in fluorescein isothiocyanate tyramide signal amplification reagent for 10 minutes in a humidity chamber, rinsed in TBS-T (3 × 3 minutes), and incubated for 30 minutes with secondary AlexaFluor 594-conjugated donkey antimouse Ab (1:50, #715-585-151; Jackson ImmunoResearch, Cambridgeshire, UK) in blocking buffer with 4′,6-diamidino-2-phenylindole (300 nM). Sections were rinsed in TBS-T (3 × 3 minutes), added 1–2 drops of Prolong Diamond (#P36961; Thermo Fisher, Waltham, Massachusetts), and cover-slipped.

Predicted LEAP2 fragments

The 77-aa prepropeptide precursor contains a typical secretory N-terminal signal sequence at amino acid position 1–22 (35). Four peptide fragments were predicted by the location of potential endoprotease cleavage sites in the precursor (amino acid sequence indicated according to precursor position). The largest mature LEAP2 form corresponds to the well-known 40-aa residue ($LEAP2_{38-77}$, ie, LEAP2) generated from the precursor at a putative cleavage site for a furin-like endoprotease (35). Three smaller peptide fragments were predicted, including a 10-aa ($LEAP2_{38-47}$), 25-aa ($LEAP2_{23-47}$), and 29-aa ($LEAP2_{49-77}$) residue.

Peptides

Peptides used in the human islet glucose-stimulated insulin secretion (GSIS) assay and mouse in vivo studies (Table 1) were synthesized at Gubra (Hørsholm, Denmark) using Fmoc-based, solid-phase peptide synthesis on a Syro II peptide synthesizer (Biotage AB, Uppsala, Sweden). Peptides were purified using reverse-phase HPLC, quantified and characterized by liquid chromatography-mass spectrometry (acquity ultra performance liquid chromatography (UPLC) equipped with a single quadrupole (SQ) detector 2 mass spectrometer; Waters, Taastrup, Denmark). The final purities of peptides were above 95%. Ghrelin was purchased from Polypeptide Inc. (Hillerød, Denmark). For the clinical study, human $LEAP2_{38-47}$ was synthetized by Bachem (Budendorf, Switzerland). The peptide was confirmed to be identical to the natural peptide by HPLC MALDI-TOF mass spectrometry, amino acid sequencing, and elemental analysis by the manufacturer. The final purity was≥97.5%.

Inositol phosphate turnover assay

COS-7 cells (ATCC CRL-1651) were cultivated in Dulbecco's modified Eagle's medium 1885 supplemented with 10% fetal bovine serum (FBS), 1% penicillin/streptomycin, and 2 mM L-glutamine at 37°C in a 10% CO_2 incubator. Cells were seeded at a density of 20 000 cells/well in a 96-well plate and allowed to attach overnight. The following day, cells were transiently transfected with pCMV-Tag2B plasmid (Stratagene, San Diego, California), either empty or containing a human growth hormone secretagogue receptor (GHSR) construct, by calcium precipitation with chloroquine at a concentration of 0.4 µg DNA/well. The GHSR construct was generated by polymerase chain reaction overlap extension with Pfu polymerase (Promega, Madison, Wisconsin), as previously described (36). The construct was verified by DNA sequencing (Eurofins MWG Operon, Ebersberg, Germany). After 5 hours, the transfection medium was changed to the cultivation medium containing 5 µL/mL of *myo*-[2-^{3}H(N)]-inositol (Perkin Elmer, Waltham, Massachusetts) and cells were then incubated for approximately 36 hours at 37°C in a 10% CO_2 incubator. Prior to the inositol phosphate accumulation assay, cells were washed

Table 1. Sequences of the largest mature LEAP2 form, smaller LEAP2 fragments and active GLP-1 (GLP-17-36) characterized in the study

Peptide	Sequence
$LEAP2_{38-77}$	H-MTPFWRGVSLRPIGASCRDDS ECITRLCRKRRCSLSVAQE-OH
$LEAP2_{38-47}$	H-MTPFWRGVSL-OH
$LEAP2_{23-47}$	H-SPIPEVSSAKRRPRRMTPFWRG VSL-OH
$LEAP2_{49-77}$	H-PIGASCRDDSECITRLCRKRRC SLSVAQE-OH
$GLP\text{-}1_{7-36}$	H-HAEGTFTSDVSSYLEGQAAKEF IAWLVKGR-NH2

once with 37°C 1 × Hanks' Balanced Salt Solution (HBSS). After washing, the cells were incubated at 37°C with 100 µl 37°C 1 × HBSS containing 10 mM LiCl and the appropriate peptide ligand at different concentrations for 90 minutes. After incubation, the plates were placed on ice and the cells were lysed with ice cold 10 mM formic acid for a minimum of 30 minutes, after which the cells were transferred to a white-bottomed 96-well plate containing scintillation proximity assay yttrium silicate beads (Perkin Elmer, Waltham, Massachusetts). The plates were shaken at maximal speed (approximately 1200 revolutions per minute) on a plate shaker for a minimum of 10 minutes at room temperature, after which the plates were spun at 1500 revolutions per minute for 5 minutes and incubated at room temperature for a minimum of 4 hours prior to measurement. Measurements were performed on a Microbeta plate reader (Perkin Elmer, Waltham, Massachusetts) using a 3-minute measuring time.

Human islet glucose-stimulated insulin secretion

All determinations of insulin secretion were performed in human pancreatic pseudoislets under static incubation. Briefly, pseudoislets were seeded into 96-well plates and preincubated for 1 hour at 37°C in Krebs-Ringer buffer (120 mM NaCl, 4 mM KCl, 2 mM $MgCl_2 \cdot 6H_2O$, 2 mM $CaCl_2 \cdot 2H_2O$, 1.19 mM $NaH_2PO_4 \cdot H_2O$, 20 mM $NaHCO_3$, and 10 mM HEPES equilibrated to pH 7.4), 0.05% BSA, and 5.6 mM glucose. The preincubation medium was then replaced with Krebs-Ringer buffer supplemented with different glucose concentrations (basal, 3 mM; stimulatory, 15 mM), as well as test compounds. The supernatant was collected after incubation for 2 hours at 37°C and the cells were then lysed in Krebs-Ringer buffer supplemented with 1.25% Triton X-100. Insulin content in supernatant and cell lysate was measured by enzyme-linked immunosorbent assay (ELISA) (Cisbio, Codolet, France) using a Tecan Envision plate reader (Tecan, Männedorf, Switzerland). Fluorescence (excitation, 320 nm; emission, 620 nm [cryptate donor emission], and 665 nm [d2 acceptor emission]) were measured twice per sample. Results were calculated ratiometrically as the 665 nm/620 nm ratio and expressed in a percentage of insulin secreted relative to total (cellular + secreted) insulin (extrapolated from standard curve) (37). Data sets from each GSIS experiment (n = 4–8 replicates per group) were pooled and repeated at least 5 times (individual donors). Data were expressed as the percentage of insulin release relative to 15 mM glucose.

Liquid chromatography-tandem mass spectrometry detection of $LEAP2_{38-47}$ in human plasma

Analyses were performed at Alphalyse (Odense, Denmark). A quantitative liquid chromatography-tandem mass spectrometry (LC-MS/MS) multiple reaction monitoring (MRM) assay was applied for determination of $LEAP2_{38-47}$ in plasma samples from randomly selected obese individuals at 3 months post-RYGB (n = 2, analysis in triplicate). To prevent degradation of $LEAP2_{38-47}$, plasma samples were mixed with phosphoric acid. External standard curves were generated by spiking human plasma samples with synthetic $LEAP2_{38-47}$ (MTPFWRGVSL). For internal standard, plasma samples were spiked with stable isotope-labeled synthetic $LEAP2_{38-47}$, carrying six ^{13}C and two $^{15}N_2$ isotopes in the arginine residue (MTPFWR[$^{13}C_6$, $^{15}N_4$]GVSL), yielding a MW of +10 Dalton compared to endogenous $LEAP2_{38-47}$. Samples were purified by Oasis HLB SPE µElution plate (Waters, Elstree, Herts, UK). All samples were dried and dissolved in 0.1% formic acid. Samples were reconstituted in a buffer containing 80% 50 mM NH_4HCO_3 and 20% acetonitrile. LC-MS/MS MRM assay conditions were as follows: HPLC, Eksigent nanoLC 400 system (SCIEX, Stockholm, Sweden); column: Acquity UPLC CSH C18 130Å 1.7 µm, 300 µm × 150 mm (Waters, Elstree, Herts, UK), flow rate 5 µL/minute, solvent A: 0.1% formic acid, solvent B: 99.9% ACN, 0.1% formic acid, injection volume 4 µL; MS/MS, Triple-TOF 6600 mass spectrometer (SCIEX, Stockholm, Sweden); ESI IonSpray voltage floating: 5500, ion source temperature 100°C, MS/MS acquisition, 100–1800 m/z. MRM data were inspected using PeakView (SCIEX, Stockholm, Sweden) and Skyline open source software. MRM transition for $LEAP2_{38-47}$ and isotopically heavy $LEAP2_{38-47}$ was 597.31 and 602.31, respectively. Peptide quantification was based on the peak area of all fragment ions of the precursor/parent ion in the extracted ion chromatogram.

Graded glucose infusion test in healthy human individuals

Ten healthy male participants were included in a randomized, double-blinded, placebo-controlled, cross-over study conducted at the Center for Clinical Metabolic Research, Gentofte Hospital, University of Copenhagen (Hellerup, Denmark). See Supplementary Figure 7 for an overview of the clinical study design (38). Informed consent was obtained from all participants before inclusion. Eligible participants were Caucasian men, aged 18–25 years, and with a body mass index of 20 to 25 kg/m^2. Exclusion criteria included anemia, history of hepatobiliary and/or gastrointestinal disorder and/or plasma liver enzymes (alanine or aspartate aminotransferases) above 2 times the normal range, serum creatinine above the normal range and/or albuminuria, first-degree and/or second-degree relatives with diabetes, tobacco smoking, and any physical or psychological condition or ongoing medication that the investigator evaluates would interfere with trial participation. Baseline characteristics of study participants are indicated

in Table 2. The study was registered at ClinicalTrials.gov (reg. no. NCT04043065). The $LEAP2_{38-47}$ was dissolved in phosphate buffer containing 0.5% human albumin (CSL Behring, Lyngby, Denmark), sterile filtrated and tested for endotoxins and sterility by the Capital Region Pharmacy (Herlev, Denmark) before dispensed into vials stored at -20°C until use. On experimental days, infusion was prepared by dilution to a total volume of 250 mL in saline (9 mg/mL, Fresenius Kabi, Uppsala, Sweden) with 0.5% human albumin. Intravenous infusion of $LEAP2_{38-47}$ (20 pmol/kg/minute) or saline (placebo) were performed on 2 experimental days in a randomized order, with a minimum of 1 week between visits. Each experimental day was preceded by 10 hours of fasting, including any liquids and 48 hours of abstinence from strenuous physical activity, medicine, alcohol, and excessive eating. A cannula was inserted in a cubital vein in each arm, 1 for peptide and glucose (20% wt/vol; Fresenius Kabi, Uppsala, Sweden) infusions and the other for blood sampling. The arm for blood sampling was wrapped in a heating pad (45°C) to arterialize the venous blood. At time point 0 minutes, the peptide or placebo infusion was started. At time point 30 minutes, the glucose infusion was initiated and adjusted to increase plasma glucose concentration, with 1.25 mM every 30 minutes from 6.25 to 11.25 mM. At time point 180 minutes, the infusions were discontinued. For bedside measurement of plasma glucose, blood was distributed in sodium fluoride-coated tubes, centrifuged immediately for 30 seconds (7600 g, room temperature), and measured by the glucose oxidase method (YSI 2900 Biochemistry Analyzer; YSI Incorporated, Yellow Springs, Ohio). Blood samples were drawn every 15 minutes. Plasma glucose was measured every 5 minutes to adjust the continuous glucose infusion. For analysis of total ghrelin, blood was collected in P800 K_2EDTA tubes containing a cocktail of protease, esterase, and dipeptidyl peptidase-4 inhibitors (#366420; BD Biosciences, San Jose, California) and immediately cooled on ice. For analysis of insulin and C-peptide, blood was collected in plain tubes with serum clot activator and left at room temperature for 20 minutes to coagulate. All tubes were centrifuged for 15 minutes (2900 g, 4°C). Plasma samples were stored at -20°C and serum samples were stored at -80°C until analysis. Plasma total ghrelin was measured by ELISA (#EZGRT-89K; Merck Millipore, Burlington, Massachusetts) according to the manufacturer's instructions. Serum insulin and C-peptide was measured using a 2-sided electrochemiluminescence immunoassay (Atellica IM Analyzer; Siemens Healthcare, Ballerup, Denmark). During experimental days, resting energy expenditure and respiratory quotient were measured by indirect calorimetry (Vyntus CPX Canopy, CareFusion, Germany) for 15 minutes at time points -20, 45, 105, and 165 minutes, with the participants in a supine position and awake. The first 5 minutes and the last 3 minutes of each measurement period were subsequently discarded. The calorimeter was calibrated before each measurement. Questionnaires about hunger, prospective food consumption, satiety, fullness, thirst, nausea, and comfort indicated on 100 mm visual analogue scales (VASs) were answered every 30 minutes (39).

Table 2. Baseline characteristics of healthy individuals in a placebo-controlled graded glucose infusion test

Male/female (n/n)	10/0
Age (years)	23 (22–24)
Weight (kg)	75.2 (69.2–84.2)
Height (m)	1.83 (1.78–1.92)
BMI (kg/m^2)	22.5 (21.9–22.8)
Fasting plasma glucose (mmol/L)	5.20 (4.88–5.43)
HbA_{1c} (mmol/mol)	30.5 (28.0–31.5)

Data are presented as median (interquartile range).
Abbreviations: BMI, body mass index; HbA1c, hemoglobin A1c.

Statistical analysis

Results are presented as mean ± standard error of mean (SEM) unless otherwise stated. Area under the curve (AUC) and baseline-subtracted AUC calculations were based on the trapezoidal rule. Fasted and postprandial plasma LEAP2 concentrations and AUC_{LEAP2} were evaluated by mixed effect repeated-measures analysis of variance (ANOVA) with Geisser-Greenhouse correction and Tukey's post hoc test. LEAP2 mRNA expression levels were analyzed by Friedman test with Dunn's post hoc test. Glucose-stimulated insulin secretion data were analyzed by a 2-way ANOVA with Dunnett's post hoc test. The graded glucose infusion test data were evaluated by a Student's paired *t*-test (baseline-subtracted AUC, baseline, peak, time to peak, and mean values). Statistical analyses were performed using GraphPad Prism v8.4.2 (GraphPad Software, San Diego, California). A *P*-value <0.05 was considered statistically significant. All supplementary material and figures are located in a digital research materials repository (38).

Results

RYGB surgery upregulates LEAP2 mRNA expression in EECs

Combined fluorescence immunostaining and LCM enabled identification and specific harvesting of EECs in gut biopsies from individuals undergoing RYGB surgery (Fig. 2A). The transcriptome analysis indicated a significant number of differentially expressed genes in postoperative mucosal biopsies compared to corresponding perioperative samples

(Fig. 2B). To extract a catalogue of differentially expressed preprohormone genes, a list of 78 known prohormone genes was compiled (34). By cross-referencing the prohormone gene catalogue with the RNAseq data set, 9 preprohormone genes were identified to be differentially regulated in the RYGB cohort as compared to perioperative expression levels (Fig. 2C). LEAP2 expression was significantly upregulated in both the biliopancreatic limb ($P = 0.0001$) and common channel ($P < 0.0001$, Fig. 2D, left panel). To confirm this finding, we performed RNAseq on LCM-harvested EECs sampled from a different cohort of individuals undergoing RYGB (24), indicating significant upregulation of LEAP2 expression in the alimentary limb ($P = 0.0070$), biliopancreatic limb ($P = 0.0008$), and common channel ($P = 0.0286$), (Fig. 2D, right panel). Subsequent ISH analyses performed on perioperative gut biopsies revealed that LEAP2 mRNA was specifically localized to intestinal cells lining the crypts (Fig. 2E). Other differentially expressed genes included *ADM* (adrenomodulin), *CCK* (cholecystokinin), *GHRH* (growth hormone releasing hormone), *GIP* (glucose-dependent insulinotropic polypeptide), *GUCA2A* (guanylate cyclase activator 2A), *MTL* (motilin), *PNOC* (prepronociceptin), and *PROK2* (prokineticin 2) (see Supplementary Figure 1) (38). We have previously reported significant upregulation of *GUCA2A* expression in EECs in individuals undergoing RYGB (37).

RYGB surgery affects plasma concentrations of LEAP2 postprandially but not in fasted condition

Using an ELISA kit previously validated for detection of the largest mature LEAP2 form ($LEAP2_{38\text{-}77}$, ie, LEAP2) in human plasma (40), we determined fasted and postprandial LEAP2 plasma concentrations 1 week before and 1 week and 3 months after RYGB surgery. Individuals undergoing RYGB surgery lost approximately 16% of their baseline body weight (121.2 ± 4.2 kg body weight 1 week before RYGB vs 102.4 ± 3.8 kg body weight 3 months after RYGB). LEAP2 fasted plasma concentration ranges were 440 to 5124 pM (2.0–21.5 ng/mL; LEAP2, MW 4581.3). RYGB surgery did not affect fasted plasma LEAP2 ($P = 0.55$, Fig. 3A) or postprandial plasma LEAP2 levels during the 3 sequential MMTs (MMTs × patient interaction, $P = 0.39$, Fig. 3B; AUC_{LEAP2}, $P = 0.19$, Fig. 3C), although we found a significant difference between MMTs performed 1 week before and after RYGB from the post hoc analyses ($P = 0.049$).

$LEAP2_{38\text{-}47}$ is a full inverse GHSR agonist

Growth hormone secretagogue receptor primarily couples through $G_{\alpha q}$, which results in phospholipase C-mediated inositol phosphate turnover (41). To characterize $LEAP2_{38\text{-}47}$ on functional GHSR activity, we determined the effect of $LEAP2_{38\text{-}47}$ on inositol phosphate accumulation in COS7 cells transfected with the human GHSR (Fig. 4A). Ghrelin stimulated inositol phosphate accumulation in GHSR-transfected COS7 cells, with an EC_{50} of 0.62 ± 0.26 nM, while LEAP2 suppressed inositol phosphate accumulation activity with an EC_{50} of 4.88 ± 0.52 nM. Similar to LEAP2, $LEAP2_{38\text{-}47}$ showed full inverse agonist activity in the inositol phosphate assay, albeit with 1000-fold lower potency (EC_{50} 2.2 ± 0.48 µM).

$LEAP2_{38\text{-}47}$ acts as an insulin secretagogue in isolated human pancreatic islets

Because an N-terminal fragment of LEAP2 has been reported to block ghrelin-induced suppression of GSIS in isolated rat pancreatic islets (29), we investigated the effect of $LEAP2_{38\text{-}47}$, $LEAP2_{23\text{-}47}$, and $LEAP2_{49\text{-}77}$ on GSIS in isolated human pancreatic islets. High glucose (15 mM) produced a significant increase in insulin secretion ($P = 0.014$) as compared to low glucose (3 mM). In a high glucose condition, human $GLP\text{-}1_{7\text{–}36}$ (0.1 µM) significantly increased insulin release, as compared to high glucose only ($P = 0.00011$). $LEAP2_{38\text{-}47}$ (1 µM) showed a significant ($P = 0.038$) increase in insulin release nearly comparable to the stimulatory effect of $GLP\text{-}1_{7\text{–}36}$ (Fig. 4B). Similar concentrations of $LEAP2_{23\text{-}47}$ and $LEAP2_{49\text{-}77}$ showed no effect on GSIS.

$LEAP2_{38\text{-}47}$ is expressed in human EECs and detectable in human plasma

Immunohistochemical analyses demonstrated expression of $LEAP2_{38\text{-}47}$ in human gut biopsies sampled perioperatively (Fig. 5A). Fluorescent double-IHC revealed that $LEAP2_{38\text{-}47}$ is expressed in most, but not all, chromogranin A (CgA)-positive cells in the human gut mucosa (Fig. 5B). An LC-MS/MS MRM assay was developed for detecting $LEAP2_{38\text{-}47}$ in human plasma samples. LC-MS/MS MRM targeted signal peaks in plasma samples spiked with synthetic, heavy $LEAP2_{38\text{-}47}$ showed the same retention time as the corresponding light endogenous $LEAP2_{38\text{-}47}$ peptide. Plasma samples from 2 randomly selected individuals undergoing RYGB were assayed for the presence of $LEAP2_{38\text{-}47}$. Plasma concentrations of $LEAP2_{38\text{-}47}$ ranged from 7.6 to 11.5 pM.

Exogenous $LEAP2_{38\text{-}47}$ has no effect on plasma glucose and insulin responses in a graded glucose infusion test in healthy human individuals

Plasma glucose concentrations and glucose infusions during the 2 experimental days are shown in Fig. 6A. Plasma and

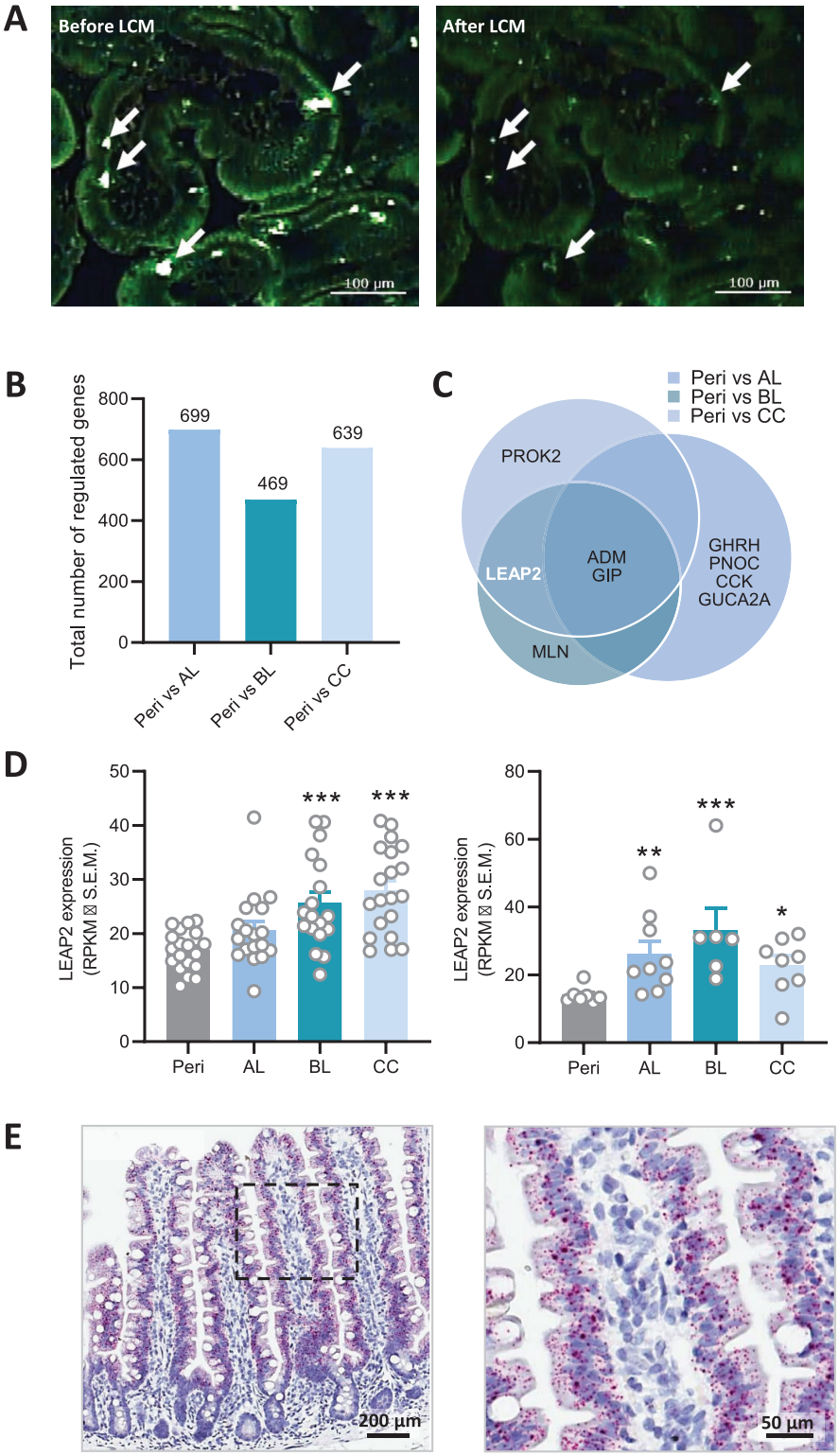

Figure 2. Human gut LEAP2 mRNA expression increases following RYGB surgery. **A:** Laser-capture microdissection (LCM) harvesting of chromogranin A (CgA)-positive enteroendocrine cells (arrows) in human gut mucosa biopsy, demonstrating selective sampling of enteroendocrine cells. A total of 1000 CgA-positive cells were collected and pooled from each biopsy for subsequent transcriptome analysis using RNAseq. Total number of differentially expressed genes (**B**) and preprohormone genes (**C**) as compared to perioperative level. **D:** mRNA expression level (RPKM ± SEM) of LEAP2. Left panel, study cohort (n = 18–20); right panel, confirmation cohort (n = 6–9). $*P < 0.05$, $**P < 0.01$, $***P < 0.001$ vs perioperative level (Friedman test with Dunn's post hoc test). **E:** In situ mRNA expression of LEAP2 in human jejunal mucosa (perioperative sample). Abbreviations: AL, alimentary limb; BL, biliopancreatic limb; CC, common channel; LEAP2, liver-expressed antimicrobial peptide 2; Peri, perioperative; RPKM, reads per kilo base per million mapped reads; RYGB, Roux-en-Y gastric bypass; SEM, standard error of mean.

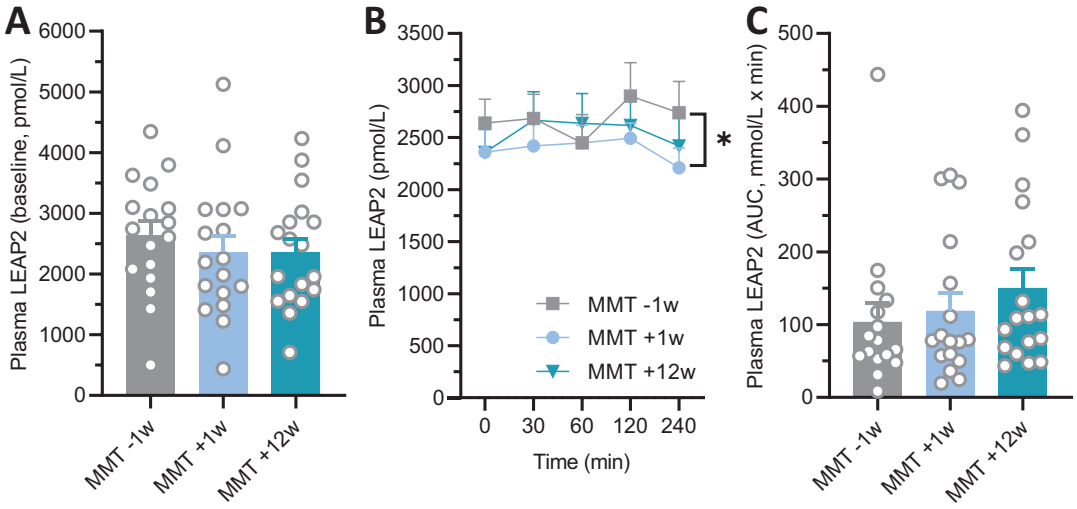

Figure 3. Circulating LEAP2 concentrations before and after RYGB surgery. Plasma concentrations of LEAP2 measured at baseline (fasted values) (**A**), during MMTs (**B**), and corresponding $AUC_{0\text{-}240\ min}$ (**C**) performed in obese individuals (n = 18) 1 week before (MMT -1 w) as well as 1 week (MMT +1 w) and 12 weeks (MMT +12 w) after RYGB. **P* < 0.05 (Tukey's post hoc test). Abbreviations: LEAP2, liver-expressed antimicrobial peptide 2; MMT, mixed meal test; RYGB, Roux-en-Y gastric bypass.

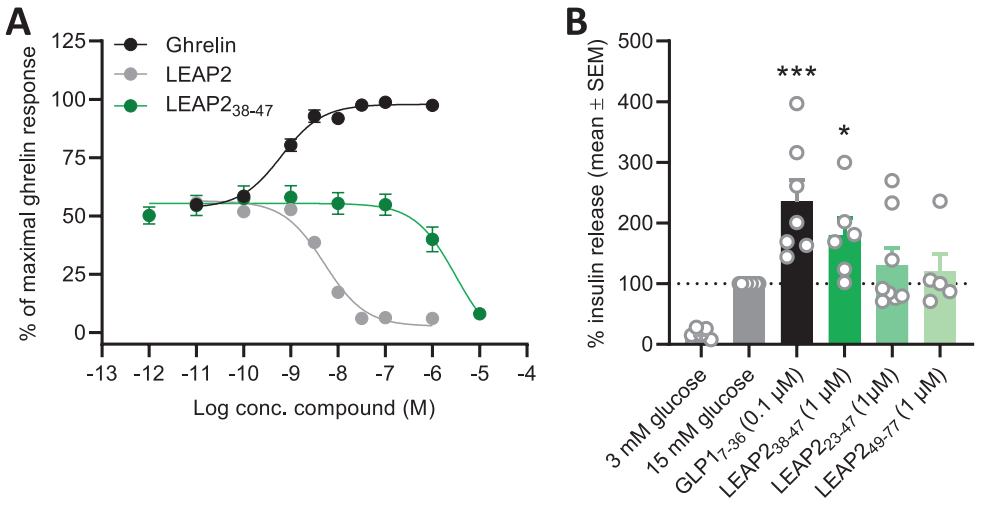

Figure 4. $LEAP2_{38\text{-}47}$, an inverse GHSR agonist and a human insulin secretagogue. **A:** LEAP2 and $LEAP2_{38\text{-}47}$ act as full inverse agonists towards human growth hormone secretagogue receptor (GHSR)-mediated constitutive phospholipase C activity in transfected COS-7 cells. The data points are depicted as the average ± SEM of 12 individual experiments for ghrelin and LEAP2 and 3 for $LEAP2_{38\text{-}47}$. The assays were performed either in duplicate or triplicate. **B:** $LEAP2_{38\text{-}47}$ augments glucose-stimulated insulin release from isolated human pancreatic pseudoislets. Data are presented as the percentage of insulin release relative to 15 mM glucose. Human GLP-17–36 (0.1 µM) was used as a positive control in the glucose-stimulated insulin secretion (GSIS) assay. **P* < 0.05, ****P* < 0.001 vs vehicle control (2-way ANOVA with Dunnett's post hoc test). Abbreviations: ANOVA, analysis of variance; LEAP2, liver-expressed antimicrobial peptide 2; SEM, standard error of mean.

serum data are indicated in Table 3. No significant differences in plasma glucose concentrations (baseline, peak, time to peak, and baseline-subtracted AUC values) during $LEAP2_{38\text{-}47}$ and placebo infusions were observed. Similar amounts of glucose ($P = 0.62$) were infused in the $LEAP2_{38\text{-}47}$ (1.19 g/kg body mass) and placebo group (1.17 g/kg body mass), respectively. Serum profiles of insulin (Fig. 6B), C-peptide:plasma glucose ratios (Fig. 6C), and plasma ghrelin concentrations (Fig. 6D) showed similar changes during $LEAP2_{38\text{-}47}$ and placebo infusions. In addition, no significant differences in resting energy expenditure or respiratory quotient between the 2 study arms at baseline or at any time interval during the glucose infusion study were observed (Supplementary Figure 2H (38)). The percent coefficient of variation (%CV) were 11.6 ± 0.57 for resting energy expenditure. Visual analogue scale (VAS) ratings of hunger, prospective food consumption, satiety, fullness, and thirst were similar during $LEAP2_{38\text{-}47}$ and placebo infusions

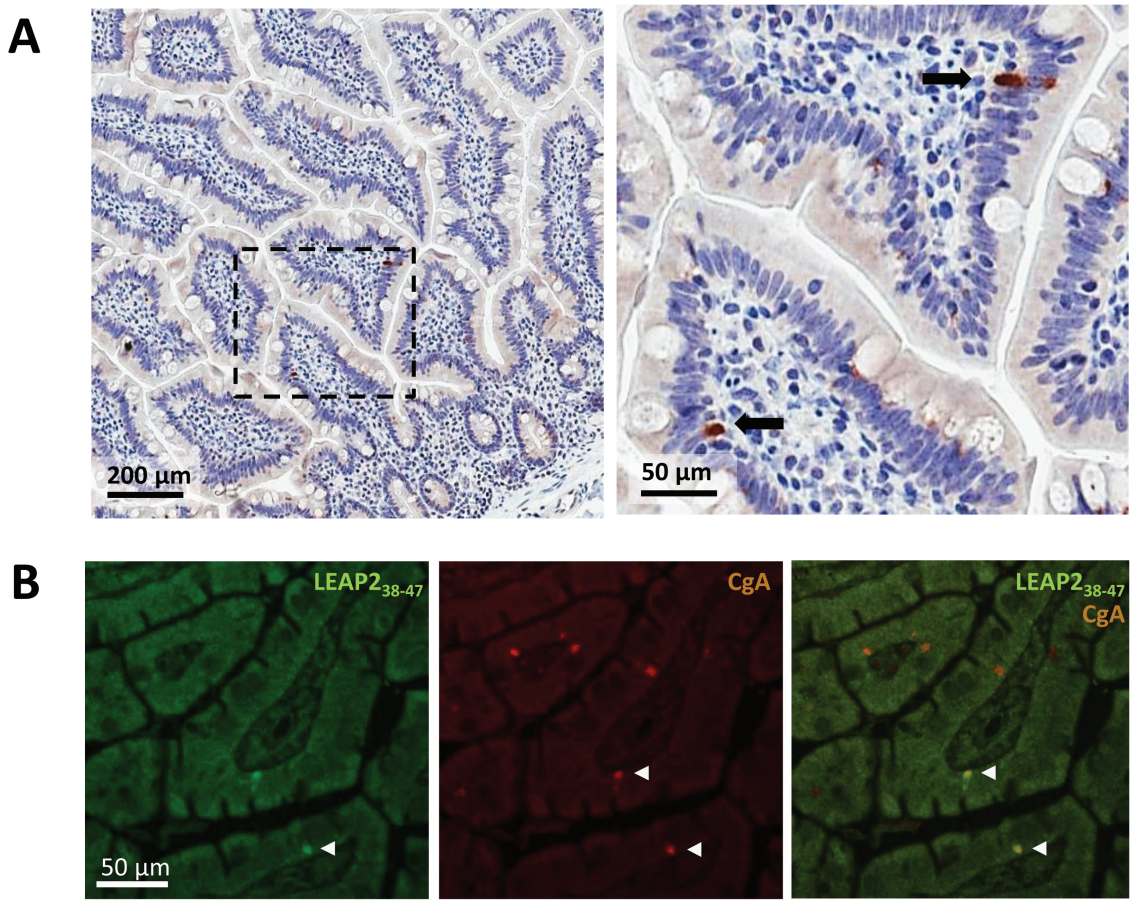

Figure 5. Distribution of LEAP2$_{38-47}$ in human gut mucosa. **A:** Immunohistochemical detection of LEAP2$_{38-47}$ expression in human jejunal mucosa (perioperative sample). **B:** Fluorescent double-immunohistochemical detection of LEAP2$_{38-47}$ peptide expression (green color) in chromogranin A (CgA)-positive enteroendocrine cells (orange color) in the human gut mucosa (perioperative sample). Arrowheads indicate cells co-expressing LEAP2$_{38-47}$ and CgA (yellow color). Abbreviation: LEAP2, liver-expressed antimicrobial peptide 2.

(Supplementary Figure 2A-E (38)). The VAS ratings indicated a high level of comfort and a low level of nausea during all interventions, and both comfort and nausea were stable over time (Supplementary Figure 2F-G (38)).

LEAP2 and LEAP2 fragment profiling in the mouse

To compare with human data, LEAP2 expression as well as metabolic effects of LEAP2 and related fragments were characterized in male NMRI mice. Using mouse-specific ISH probes, LEAP2 mRNA expression was clearly detected in the gut epithelial layer. Whereas jejunal samples showed highest expression level, LEAP2 mRNA was virtually absent in the colon (Supplementary Figure 3A (38)). Similar to humans, murine LEAP2$_{38-47}$ expression was specifically localized to the gut epithelium (Supplementary Figure 3B (38)). Effects of human LEAP2 fragments on real-time food intake and oral glucose tolerance were assessed in chow-fed NMRI mice following single subcutaneous (s.c.) dosing. Human GLP-1$_{7-36}$ (3000 nmol/kg, s.c.) promoted a significant drop in cumulative food intake during the 6-hour monitoring period as compared to vehicle dosing. In contrast, a similar dose of LEAP2, LEAP2$_{38-47}$, LEAP2$_{23-47}$, and LEAP2$_{49-77}$ did not affect cumulative food intake (Supplementary Figure 4 (38)). Whereas a relatively low dose of human GLP-1$_{7-36}$ (300 nmol/kg, s.c.) significantly reduced baseline blood glucose concentrations and glucose excursions in an oral glucose tolerance test, LEAP2, LEAP2$_{38-47}$, LEAP2$_{23-47}$, and LEAP2$_{49-77}$ showed no effect on glucose homeostasis in NMRI mice (Supplementary Figure 5 (38)). In addition, LEAP2$_{38-47}$ was characterized on GSIS in isolated mouse pancreatic islets. During high-glucose condition, human GLP-1$_{7-36}$ (0.1 µM) significantly increased GSIS compared to high-glucose only (P = 0.0035). In contrast, LEAP2$_{38-47}$ (3 µM) did not influence GSIS (Supplementary Figure 6 (38)).

Discussion

LEAP2 has been proposed as a signaling peptide that regulates energy homeostasis through its reciprocal relationship

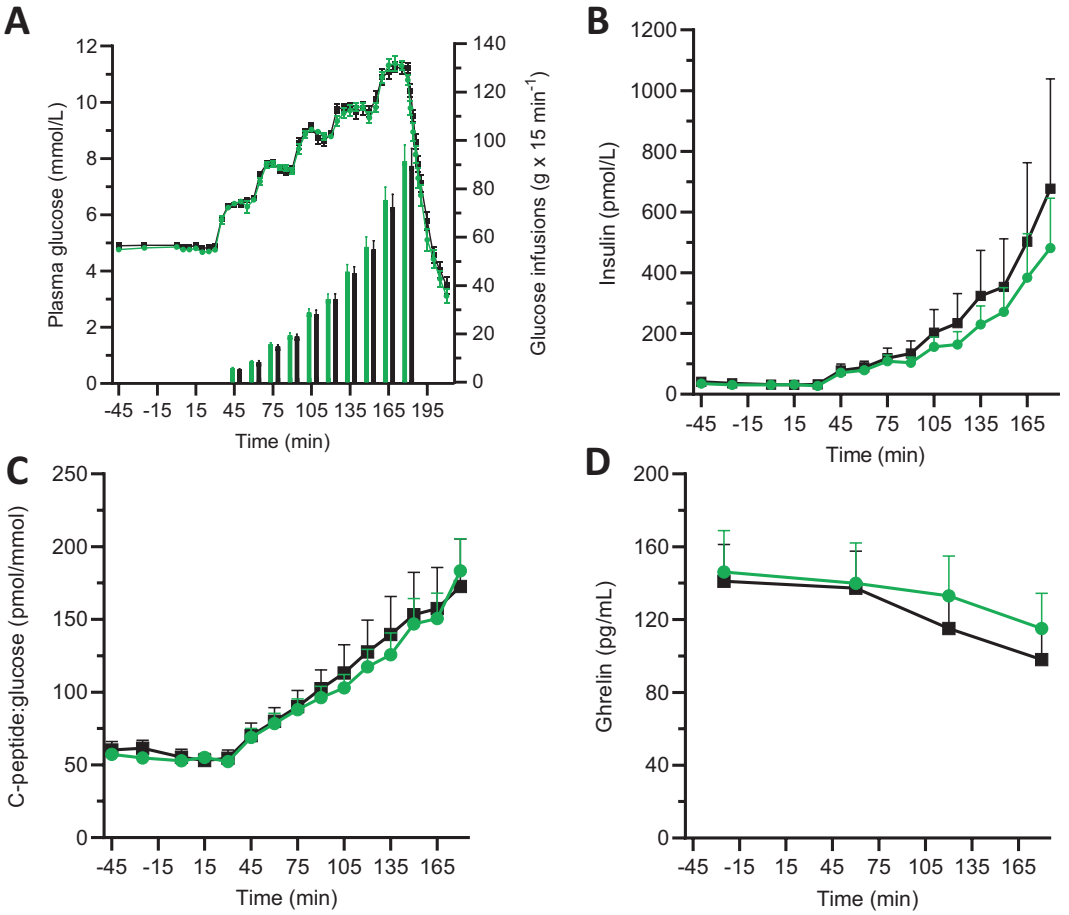

Figure 6. $LEAP2_{38-47}$ does not affect glucose and insulin levels in a graded glucose infusion test in healthy human individuals. **A:** Plasma glucose concentrations and concomitant glucose infusions (depicted as bar graphs in grams per 15-minute time intervals). Serum concentrations of insulin (**B**) and C-peptide:plasma glucose ratios (**C**). **D:** Plasma concentrations of ghrelin. Green round symbols, $LEAP2_{38-47}$ infusion; black square symbols, placebo (n = 10). No significant differences (Student's paired *t*-test of baseline-subtracted AUC, baseline, peak, time to peak, and mean [only F] values). Abbreviations: AUC, area under the curve; LEAP2, liver-expressed antimicrobial peptide 2.

to the appetite-promoting stomach hormone ghrelin (28). Here, we report elevated LEAP2 expression in human EECs following RYGB surgery. Notably, a secreted endogenous LEAP2 fragment showed insulinotropic properties in vitro; however, with no glucoregulatory effect in a clinical proof-of-concept trial in the dose chosen. LEAP2 mRNA expression in EECs was significantly increased following RYGB compared to perioperative expression levels. Increased LEAP2 expression was further confirmed in EECs from a separate cohort of individuals undergoing RYGB. ISH indicated that LEAP2 mRNA is not restricted to the EECs but densely expressed in gut epithelial cells lining the crypts, being in agreement with previous LEAP2 IHC studies on human colon samples (42, 43).

The upregulation of LEAP2 gene expression in EECs prompted us to investigate circulating LEAP2 concentrations before and after RYGB. Because both fasting and postprandial levels of other gut hormones such as GLP-1 and peptide YY have been reported elevated after RYGB (6, 13, 44), we determined plasma LEAP2 concentrations in MMTs performed 1 week before as well as 1 week and 3 months after RYGB. LEAP2 was detected in plasma samples from individuals undergoing RYGB, being within concentration ranges reported in a recent clinical study by Mani et al (40). Hence, our data confirms that LEAP2 is processed to its mature form and secreted into circulation. Compared to presurgery, both fasting and postprandial plasma LEAP2 concentrations remained unaltered up to 3 months after RYGB, although we found a slight decrease in plasma LEAP2 during the MMT performed 1 week after RYGB, ie, before any significant weight loss was achieved. In combination with the robust RYGB-induced weight loss 3 months postoperative, this suggests that LEAP2 levels may not be sensitive to weight loss. We cannot rule out that secretion from other enterocyte cell populations and/or organs with high LEAP2 expression, in particular the liver (35), could potentially have masked any potential changes in gut-derived LEAP2 secretion. It should be noted

Table 3. Plasma and serum measurements from healthy individuals in a placebo-controlled graded glucose infusion test

	$LEAP2_{38-47}$	Placebo (Saline)
Plasma glucose		
Baseline (mmol/L)	4.82 ± 0.0690	4.91 ± 0.0689
Peak (mmol/L)	11.9 ± 0.174	11.8 ± 0.107
Time to peak (min)	168 ± 1.71	171 ± 2.45
bsAUC (mmol/L × min)	592 ± 23.7	597 ± 24.2
Serum insulin		
Baseline (pmol/L)	32.2 ± 3.19	36.3 ± 5.39
Peak (pmol/L)	483 ± 164	680 ± 362
Time to peak (min)	179 ± 1.50	177 ± 2.00
bsAUC (nmol/L × min)	22.6 ± 7.23	30.5 ± 14.9
Serum C-peptide		
Baseline (pmol/L)	265 ± 17.1	290 ± 27.7
Peak (pmol/L)	1985 ± 259	1970 ± 399
Time to peak (min)	180 ± 0	180 ± 0
bsAUC (nmol/L × min)	107 ± 14.8	111 ± 23.1
C-peptide:glucose ratio		
Baseline (pmol/mmol)	55.0 ± 3.28	59.0 ± 5.49
Peak (pmol/mmol)	183 ± 22.2	174 ± 32.7
Time to peak (min)	180 ± 0	179 ± 1.50
bsAUC (nmol/mmol × min)	8.13 ± 1.42	8.29 ± 2.18
Plasma ghrelin		
Baseline (pg/mL)	146 ± 22.8	141 ± 20.2
Peak (pg/mL)	150 ± 21.9	143 ± 20.2
Time to peak (min)	12.5 ± 19.8	23.5 ± 17.1
bsAUC (pg/mL × min)	-2584 ± 812	-3121 ± 635

No significant differences (Student's paired t-test).
Abbreviations: bsAUC, baseline subtracted area under the curve; LEAP2, liver-expressed antimicrobial peptide 2; min, minutes.

that Mani et al reported lowered fasting plasma LEAP2 concentrations at the 2-year follow-up (40), making it possible that LEAP2 is regulated by more long-term metabolic changes following RYGB. Mani et al also demonstrated reductions in LEAP2 levels at the 2-hour time point during an MMT performed at 3 months after RYGB. In contrast, we did not observe MMT-evoked effects on plasma LEAP2 concentrations at both 1 week or 3 months postoperatively. As we used a lower caloric challenge (300 kcal) compared to Mani et al (600 kcal), this leaves it presently unresolved if LEAP2 is regulated by RYGB-induced weight loss after a nutrient challenge.

A pioneering study characterizing human LEAP2 expression demonstrated the presence of smaller circulating LEAP2 peptide fragments in human blood ultrafiltrates, which could indicate proteolytic processing of the precursor peptide and/or LEAP2 (35). To date, degradation products of these peptides have not been described with respect to potential biological activity. This prompted us to characterize putative degradation products based on the position of putative peptidase cleavage sites in the precursor peptide. In addition to LEAP2, 3 smaller peptide fragments were predicted, ie, $LEAP2_{38-47}$, $LEAP2_{23-47}$, and $LEAP2_{49-77}$. Of the smaller fragments, only $LEAP2_{38-47}$ augmented GSIS in isolated human pancreatic islets, promoting an increase in insulin release nearly comparable to $GLP\text{-}1_{7-36}$, indicating insulin secretagogue properties of $LEAP2_{38-47}$. An N-terminal modified, structurally related LEAP2 residue has been reported to block ghrelin-induced suppression of GSIS in rat pancreatic islets without showing GSIS stimulatory effect per se (29), possibly suggesting different receptor binding properties or species differences in the modulatory action of GHSR on insulin secretion. The latter is supported by our observation that $LEAP2_{38-47}$ did not enhance GSIS in an isolated mouse islet assay. LEAP2 is an inverse agonist for GHSR (29), the cognate receptor for ghrelin (45). The N-terminal part of mature LEAP2, encompassing at least the 1–8 aa residue ($LEAP_{38-45}$), confers GHSR binding and inverse agonist activity, which likely explains why $LEAP2_{49-77}$ lacked GSIS activity. As we only tested a single concentration (1 µM) of each LEAP2 fragment, it remains to be determined if $LEAP2_{23-47}$ may be a weaker insulin secretagogue compared to $LEAP2_{38-47}$. Using COS-7 cells transiently transfected with the human GHSR, we confirmed that ghrelin and LEAP2 show reciprocal effects on constitutive GHSR activity. Similar to LEAP2, $LEAP2_{38-47}$ was a full GHSR inverse agonist as demonstrated by reduced basal inositol phosphate turnover, albeit with significantly lower potency. The human pancreas shows high GHSR expression, particular in somatostatin-producing delta cells (46, 47). Mouse islet cell transcriptome studies have unequivocally established that GHSR expression is extremely low in alpha cells and absent in beta cells (48, 49). Delta cell-selective expression of GHSR is consistent with the finding that ghrelin potentiates glucose-stimulated somatostatin secretion in mouse and human islets, making it conceivable that the well-known insulinostatic effect of ghrelin is indirect to delta cell-mediated local inhibitory feedback (48, 50). Taken together, this suggests that insulinotropic action of $LEAP2_{38-47}$ may be directly linked to attenuation of tonic GHSR activity.

Subsequently, IHC analyses on perioperative biopsies demonstrated that $LEAP2_{38-47}$ was expressed in some, but not all, CgA-positive cells. The occurrence of $LEAP2_{38-47}$ expression in discrete EECs contrasts the dense expression of LEAP2 mRNA in intestinal epithelial cells. Apart from differences in assay sensitivity, the different distribution pattern suggests that the prepropeptide precursor is not fully processed to $LEAP2_{38-47}$ in all EECs. Interestingly, the LEAP2 gene has been reported to undergo alternative splicing, which is predicted to produce an array of distinct but structurally related peptides that may be secreted

or retained within the cell (35, 42). While EECs constitute a highly specialized mucosal cell subpopulation, the enteroendocrine lineage consists of several secretory cell types that differ on the basis of their morphology, specific regional distribution and peptide expression pattern (51, 52). Future studies must therefore aim to address whether LEAP2 and related isoforms may be expressed in different intestinal epithelial cell lineages.

Given the specific expression of $LEAP2_{38-47}$ in human EECs, we isolated $LEAP2_{38-47}$ in plasma samples from 2 individuals undergoing RYGB. The $LEAP2_{38-47}$ peptide was detected in both samples, albeit at low concentrations, demonstrating that $LEAP2_{38-47}$ is a human endogenous, circulating peptide. The large difference in plasma concentrations of $LEAP2_{38-47}$ (picomolar range) and LEAP2 (nanomolar range) could potentially signify that $LEAP2_{38-47}$ is not a major endogenous metabolite of LEAP2. However, it should be taken into account that other gut-derived peptide hormones such as GLP-1 and peptide YY are secreted in picomolar amounts and rapidly inactivated by peptidases and cleared from systemic circulation (53, 54), which may also apply to $LEAP2_{38-47}$. The low plasma concentrations of $LEAP2_{38-47}$ also invite the possibility that this peptide hormone may predominantly have paracrine effects in the gut.

The insulinotropic actions of $LEAP2_{38-47}$ in isolated human pancreatic islets could potentially translate to glucoregulatory effects. In a clinical proof-of-concept trial including healthy male individuals, we sought to investigate the glycemic effect of $LEAP2_{38-47}$ in a graded glucose infusion test. Importantly, no adverse reactions were observed during infusions with $LEAP2_{38-47}$. $LEAP2_{38-47}$ did not influence glucose and insulin responses in the chosen dose. Moreover, no effect on plasma ghrelin or resting energy expenditure was found. Limitations of the study should be considered. We did not determine plasma $LEAP2_{38-47}$ concentrations during infusions, leaving it uncertain if $LEAP2_{38-47}$ was rapidly degraded before reaching the target. Analyses of human $LEAP2_{38-47}$ pharmacokinetics are therefore warranted. Also, it may be possible that co-infusion with ghrelin and $LEAP2_{38-47}$ during glucose administration is more suitable for addressing any potential glucoregulatory effects of $LEAP2_{38-47}$.

A series of mouse studies were conducted to further address potential metabolic effects of $LEAP2_{38-47}$. Similar to human gut biopsies, LEAP2 mRNA expression was clearly identified in the mouse gut epithelial layer, being highest within the jejunum. The gut distribution and epithelial localization of LEAP2 gene expression is in close agreement with previously reported data in the mouse (28). Correspondingly, $LEAP2_{38-47}$ peptide expression was detected within the mouse gut epithelial layer. In contrast to the administration of $GLP\text{-}1_{7-36}$, we observed no effect on oral glucose tolerance and food intake following single dosing of LEAP2 and $LEAP2_{38-47}$ in chow-fed mice. LEAP2 and related peptide fragments were administered at a high dose (3000 nmol/kg), indicating that these peptides are not displaying glucoregulatory or appetite suppressing effects per se in normoglycemic, lean mice. Few studies on LEAP2 pharmacology have previously been reported in mice. As LEAP2 and a truncated variant has been demonstrated to reverse ghrelin-induced hyperphagia in mice (28, 29), this could point to that metabolic activity of LEAP2 family peptides may depend on supraphysiological GHSR activity. Because ghrelin exerts its orexigenic action by stimulating central GHSR activity (55), limited central nervous system (CNS) accessibility of LEAP2 and related peptide fragments following systemic administration may potentially explain the lack of acute food intake responses in lean mice. It also remains to be determined if LEAP2-family peptides may show effects in conditions of poor metabolic control, making it relevant in future studies to profile these peptides in animal models of diet-induced obesity or type 2 diabetes.

In conclusion, the present study assessed the preprohormone gene expression profile in isolated EECs from human obese individuals undergoing RYGB surgery. While LEAP2 expression was consistently increased following RYGB, this effect did not translate into changes in systemic circulating LEAP2 concentrations in individuals undergoing RYGB. $LEAP2_{38-47}$ was identified as a human endogenous LEAP2-related peptide fragment with insulin secretagogue properties in vitro, but did not exhibit glucoregulatory effects in a clinical proof-of-concept trial. Whether other LEAP2 family peptide hormones may be targets for the treatment of diabetes remains to be investigated.

Acknowledgments

We thank the staff at Gentofte Hospital, Sanofi Aventis and Gubra for assistance with performing the experiments.

Financial Support: This work was supported by Innovation Fund Denmark (C.A.H., C.Z.) and Sanofi-Aventis (Frankfurt, Germany).

Clinical Trial Information: Clinical trial registration numbers: H-6-2014-047 and H-18027152.

Author Contributions: C.A.H., C.Z., T.J., N.C.B., T.V., B.H., N.V., J.J., and F.K.K. contributed to the design of the study. C.A.H., C.Z., T.J., K.T.R., M.R.M., S.M.H., M.C., M.F., S.T., S.H., and M.A.H. conducted the experiments and/or analyzed data. C.A.H., C.Z., H.H.H., J.J., and F.K.K. wrote the manuscript. B.H., J.J., and F.K.K. supervised the research activity. All authors critically revised and approved the final version of the manuscript.

Additional Information

Correspondence and Reprint Requests: F. K. Knop, Center for Clinical Metabolic Research, Gentofte Hospital, University of Co-

penhagen, Gentofte Hospitalsvej 7, 3rd floor, DK-2900 Hellerup, Denmark. E-mail: filip.krag.knop.01@regionh.dk.

Disclosure Summary. N.V. and J.J. are owners of Gubra. F.K.K. has served on scientific advisory panels and/or been part of speaker's bureaus for, served as a consultant to, and/or received research support from Amgen, AstraZeneca, Boehringer Ingelheim, Carmot Therapeutics, Eli Lilly, Gubra, MedImmune, MSD/Merck, Mundipharma, Norgine, Novo Nordisk, Sanofi, and Zealand Pharma. All other authors have nothing to declare.

Data Availability: All data generated or analyzed during this study are included in this published article or in the data repositories listed in References.

References

1. Buchwald H, Estok R, Fahrbach K, et al. Weight and type 2 diabetes after bariatric surgery: systematic review and meta-analysis. *Am J Med*. 2009;**122**(3):248–256.e5.
2. Schauer PR, Bhatt DL, Kirwan JP, et al.; STAMPEDE Investigators. Bariatric surgery versus intensive medical therapy for diabetes – 5-year outcomes. *N Engl J Med*. 2017;**376**(7):641–651.
3. Sjöström L, Peltonen M, Jacobson P, et al. Bariatric surgery and long-term cardiovascular events. *JAMA*. 2012;**307**(1):56–65.
4. Steven S, Hollingsworth KG, Small PK, et al. Calorie restriction and not glucagon-like peptide-1 explains the acute improvement in glucose control after gastric bypass in Type 2 diabetes. *Diabet Med*. 2016;**33**(12):1723–1731.
5. Bojsen-Møller KN, Dirksen C, Jørgensen NB, et al. Early enhancements of hepatic and later of peripheral insulin sensitivity combined with increased postprandial insulin secretion contribute to improved glycemic control after Roux-en-Y gastric bypass. *Diabetes*. 2014;**63**(5):1725–1737.
6. Jacobsen SH, Olesen SC, Dirksen C, et al. Changes in gastrointestinal hormone responses, insulin sensitivity, and beta-cell function within 2 weeks after gastric bypass in non-diabetic subjects. *Obes Surg*. 2012;**22**(7):1084–1096.
7. Narath SH, Mautner SI, Svehlikova E, et al. An untargeted metabolomics approach to characterize short-term and long-term metabolic changes after bariatric surgery. *PLoS One*. 2016;**11**(9):e0161425.
8. Li QR, Wang ZM, Wewer Albrechtsen NJ, et al. Systems signatures reveal unique remission-path of type 2 diabetes following Roux-en-Y gastric bypass surgery. *Ebiomedicine*. 2018;**28**:234–240.
9. Patti ME, Houten SM, Bianco AC, et al. Serum bile acids are higher in humans with prior gastric bypass: potential contribution to improved glucose and lipid metabolism. *Obesity (Silver Spring)*. 2009;**17**(9):1671–1677.
10. Palleja A, Kashani A, Allin KH, et al. Roux-en-Y gastric bypass surgery of morbidly obese patients induces swift and persistent changes of the individual gut microbiota. *Genome Med*. 2016;**8**(1):67.
11. Martin AM, Sun EW, Keating DJ. Mechanisms controlling hormone secretion in human gut and its relevance to metabolism. *J Endocrinol*. 2019;**244**(1):R1–R15.
12. Gribble FM, Reimann F. Enteroendocrine cells: chemosensors in the intestinal epithelium. *Annu Rev Physiol*. 2016;**78**:277–299.
13. Dirksen C, Jørgensen NB, Bojsen-Møller KN, et al. Gut hormones, early dumping and resting energy expenditure in patients with good and poor weight loss response after Roux-en-Y gastric bypass. *Int J Obes (Lond)*. 2013;**37**(11):1452–1459.
14. Jorsal T, Rhee NA, Pedersen J, et al. Enteroendocrine K and L cells in healthy and type 2 diabetic individuals. *Diabetologia*. 2018;**61**(2):284–294.
15. Moffett RC, Docherty NG, le Roux CW. The altered enteroendocrine reportoire following roux-en-Y-gastric bypass as an effector of weight loss and improved glycaemic control. *Appetite*. 2020;**156**:104807.
16. Nielsen MS, Ritz C, Wewer Albrechtsen NJ, Holst JJ, le Roux CW, Sjödin A. Oxyntomodulin and glicentin may predict the effect of bariatric surgery on food preferences and weight loss. *J Clin Endocrinol Metab*. 2020;**105**(4):E1064–E1074.
17. Xu HC, Pang YC, Chen JW, et al. Systematic review and meta-analysis of the change in ghrelin levels after Roux-en-Y gastric bypass. *Obes Surg*. 2019;**29**(4):1343–1351.
18. Schmidt JB, Pedersen SD, Gregersen NT, et al. Effects of RYGB on energy expenditure, appetite and glycaemic control: a randomized controlled clinical trial. *Int J Obes (Lond)*. 2016;**40**(2):281–290.
19. Roth CL, Reinehr T, Schernthaner GH, Kopp HP, Kriwanek S, Schernthaner G. Ghrelin and obestatin levels in severely obese women before and after weight loss after Roux-en-Y gastric bypass surgery. *Obes Surg*. 2009;**19**(1):29–35.
20. Martins C, Kjelstrup L, Mostad IL, Kulseng B. Impact of sustained weight loss achieved through Roux-en-Y gastric bypass or a lifestyle intervention on ghrelin, obestatin, and ghrelin/obestatin ratio in morbidly obese patients. *Obes Surg*. 2011;**21**(6):751–758.
21. Behary P, Tharakan G, Alexiadou K, et al. Combined GLP-1, oxyntomodulin, and peptide YY improves body weight and glycemia in obesity and prediabetes/type 2 diabetes: a randomized, single-blinded, placebo-controlled study. *Diabetes Care*. 2019;**42**(8):1446–1453.
22. Tan T, Behary P, Tharakan G, et al. The effect of a subcutaneous infusion of GLP-1, OXM, and PYY on energy intake and expenditure in obese volunteers. *J Clin Endocrinol Metab*. 2017;**102**(7):2364–2372.
23. Hope DCD, Tan TMM, Bloom SR. No guts, no loss: toward the ideal treatment for obesity in the twenty-first century. *Front Endocrinol (Lausanne)*. 2018;**9**:442.
24. Rhee NA, Wahlgren CD, Pedersen J, et al. Effect of Roux-en-Y gastric bypass on the distribution and hormone expression of small-intestinal enteroendocrine cells in obese patients with type 2 diabetes. *Diabetologia*. 2015;**58**(10):2254–2258.
25. Hansen CF, Bueter M, Theis N, et al. Hypertrophy dependent doubling of L-cells in Roux-en-Y gastric bypass operated rats. *PLoS One*. 2013;**8**(6):e65696.
26. Nergård BJ, Lindqvist A, Gislason HG, et al. Mucosal glucagon-like peptide-1 and glucose-dependent insulinotropic polypeptide cell numbers in the super-obese human foregut after gastric bypass. *Surg Obes Relat Dis*. 2015;**11**(6):1237–1246.
27. Mumphrey MB, Patterson LM, Zheng H, Berthoud HR. Roux-en-Y gastric bypass surgery increases number but not density of CCK-, GLP-1-, 5-HT-, and neurotensin-expressing enteroendocrine cells in rats. *Neurogastroenterol Motil*. 2013;**25**(1):e70–e79.

28. Ge X, Yang H, Bednarek MA, et al. LEAP2 is an endogenous antagonist of the ghrelin receptor. *Cell Metab*. 2018;**27**(2):461–469.e6.
29. M'Kadmi C, Cabral A, Barrile F, et al. N-terminal liver-expressed antimicrobial peptide 2 (LEAP2) region exhibits inverse agonist activity toward the ghrelin receptor. *J Med Chem*. 2019;**62**(2):965–973.
30. Christensen MM, Jorsal T, Mortensen B, et al. The effect of Roux-en-Y gastric bypass surgery on the gut mucosal gene expression profile and circulating gut hormones. *Diabetologia*. 2018;**61**(Suppl 1):248–249, 508.
31. Facer P, Bishop AE, Lloyd RV, Wilson BS, Hennessy RJ, Polak JM. Chromogranin: a newly recognized marker for endocrine cells of the human gastrointestinal tract. *Gastroenterology*. 1985;**89**(6):1366–1373.
32. Zhang C, Rigbolt K, Petersen SL, et al. The preprohormone expression profile of enteroendocrine cells following Roux-en-Y gastric bypass in rats. *Peptides*. 2019;**118**:170100.
33. Love MI, Huber W, Anders S. Moderated estimation of fold change and dispersion for RNA-seq data with DESeq2. *Genome Biol*. 2014;**15**(12):550.
34. Hagemann CA, Zhang C, Hansen HH, et al. Data from: Identification and metabolic profiling of a novel human gut-derived LEAP2 fragment. Gene Expression Omnibus (GEO) database. Deposited November 18, 2020. ProMEDmail website. https://www.ncbi.nlm.nih.gov/geo/query/acc.cgi?acc=GSE154306.
35. Krause A, Sillard R, Kleemeier B, et al. Isolation and biochemical characterization of LEAP-2, a novel blood peptide expressed in the liver. *Protein Sci*. 2003;**12**(1):143–152.
36. Mokrosiński J, Frimurer TM, Sivertsen B, Schwartz TW, Holst B. Modulation of constitutive activity and signaling bias of the ghrelin receptor by conformational constraint in the second extracellular loop. *J Biol Chem*. 2012;**287**(40):33488–33502.
37. Fernandez-Cachon ML, Pedersen SL, Rigbolt KT, et al. Guanylin and uroguanylin mRNA expression is increased following Roux-en-Y gastric bypass, but guanylins do not play a significant role in body weight regulation and glycemic control. *Peptides*. 2018;**101**:32–43.
38. Hagemann CA, Zhang C, Hansen HH, et al. Data from: Identification and metabolic profiling of a novel human gutderived LEAP2 fragment. Figshare Repository. Deposited November 18, 2020. ProMEDmail website. https://doi.org/10.6084/m9.figshare.12789353.
39. Flint A, Raben A, Blundell JE, Astrup A. Reproducibility, power and validity of visual analogue scales in assessment of appetite sensations in single test meal studies. *Int J Obes Relat Metab Disord*. 2000;**24**(1):38–48.
40. Mani BK, Puzziferri N, He Z, et al. LEAP2 changes with body mass and food intake in humans and mice. *J Clin Invest*. 2019;**129**(9):3909–3923.
41. M'Kadmi C, Leyris JP, Onfroy L, et al. Agonism, antagonism, and inverse agonism bias at the ghrelin receptor signaling. *J Biol Chem*. 2015;**290**(45):27021–27039.
42. Howard A, Townes C, Milona P, Nile CJ, Michailidis G, Hall J. Expression and functional analyses of liver expressed antimicrobial peptide-2 (LEAP-2) variant forms in human tissues. *Cell Immunol*. 2010;**261**(2):128–133.
43. Shata MT, Abdel-Hameed EA, Hetta HF, Sherman KE. Immune activation in HIV/HCV-infected patients is associated with low-level expression of liver expressed antimicrobial peptide-2 (LEAP-2). *J Clin Pathol*. 2013;**66**(11):967–975.
44. le Roux CW, Welbourn R, Werling M, et al. Gut hormones as mediators of appetite and weight loss after Roux-en-Y gastric bypass. *Ann. Surg*. 2007;**246**(5):780–785.
45. Howard AD, Feighner SD, Cully DF, et al. A receptor in pituitary and hypothalamus that functions in growth hormone release. *Science*. 1996;**273**(5277):974–977.
46. Gnanapavan S, Kola B, Bustin SA, et al. The tissue distribution of the mRNA of ghrelin and subtypes of its receptor, GHS-R, in humans. *J Clin Endocrinol Metab*. 2002;**87**(6):2988–2991.
47. Lawlor N, George J, Bolisetty M, et al. Single-cell transcriptomes identify human islet cell signatures and reveal cell-type-specific expression changes in type 2 diabetes. *Genome Res*. 2017;**27**(2):208–222.
48. Adriaenssens AE, Svendsen B, Lam BY, et al. Transcriptomic profiling of pancreatic alpha, beta and delta cell populations identifies delta cells as a principal target for ghrelin in mouse islets. *Diabetologia*. 2016;**59**(10):2156–2165.
49. DiGruccio MR, Mawla AM, Donaldson CJ, et al. Comprehensive alpha, beta and delta cell transcriptomes reveal that ghrelin selectively activates delta cells and promotes somatostatin release from pancreatic islets. *Mol Metab*. 2016;**5**(7):449–458.
50. Kurashina T, Dezaki K, Yoshida M, et al. The β-cell GHSR and downstream cAMP/TRPM2 signaling account for insulinostatic and glycemic effects of ghrelin. *Sci Rep*. 2015;**5**:14041.
51. Engelstoft MS, Egerod KL, Lund ML, Schwartz TW. Enteroendocrine cell types revisited. *Curr Opin Pharmacol*. 2013;**13**(6):912–921.
52. Gunawardene AR, Corfe BM, Staton CA. Classification and functions of enteroendocrine cells of the lower gastrointestinal tract. *Int J Exp Pathol*. 2011;**92**(4):219–231.
53. Holst JJ, Deacon CF. Glucagon-like peptide-1 mediates the therapeutic actions of DPP-IV inhibitors. *Diabetologia*. 2005;**48**(4):612–615.
54. Toräng S, Bojsen-Møller KN, Svane MS, et al. In vivo and in vitro degradation of peptide YY3–36 to inactive peptide YY3–34 in humans. *Am J Physiol*. 2016;**310**(9):R866–R874.
55. Fry M, Ferguson AV. Ghrelin: Central nervous system sites of action in regulation of energy balance. *Int J Pept*. 2010;**2010**:616757.